



The expression and functional analysis of the sialyl-T antigen in prostate cancer

Ruifeng Bai¹ · Xue Luan¹ · Yu Zhang¹ · Catherine Robbe-Masselot² · Inka Brockhausen³ · Yin Gao^{1,3} 

Received: 8 October 2019 / Revised: 4 May 2020 / Accepted: 12 May 2020
© Springer Science+Business Media, LLC, part of Springer Nature 2020

Abstract

Aberrant glycosylation is a featured characteristic of cancer and plays a role in cancer pathology; thus an understanding of the compositions and functions of glycans is critical for discovering diagnostic biomarkers and therapeutic targets for cancer. In this study, we used MALDI-TOF-MS analysis to determine the *O*-glycan profiles of prostate cancer cells metastasized to bone (PC-3), brain (DU145), lymph node (LNCaP), and vertebra (VCaP) in comparison to immortalized RWPE-1 cells derived from normal prostatic tissue. Prostate cancer (CaP) cells exhibited an elevation of simple/short *O*-glycans, with a reduction of complex *O*-glycans, increased *O*-glycan sialylation and decreased fucosylation. Core 1 sialylation was increased dramatically in all CaP cells, and especially in PC-3 cells. The expression of Neu5Ac α 2-3Gal β 1-3GalNAc- (sialyl-3T antigen) which is the product of α 2,3-sialyltransferase-I (ST3Gal-I) was substantially increased. We therefore focused on exploring the possible function of ST3Gal-I in PC-3 cells. ST3Gal-I silencing studies showed that ST3Gal-I was associated with PC-3 cell proliferation, migration and apoptosis. Further *in vivo* studies demonstrated that down regulation of ST3Gal-I reduced the tumor size in xenograft mouse model, indicating that sialyl-3T can serve as a biomarker for metastatic prostate cancer prognosis, and that ST3Gal-I could be a target for therapeutic intervention in cancer treatment.

Keywords Prostate cancer · Glycosylation · Mass spectrometry · α 2,3-sialyltransferase · Sialyl-3T antigen

Introduction

Prostate cancer (CaP) is one of the most commonly diagnosed cancers in men and a major cause of cancer death worldwide [1]. Being a heterogeneous disease, CaP displays a variety of clinical phenotypes, among which up to 20% develop to more aggressive and metastatic states, frequently with metastasis to

bone, brain, lymph node and vertebra, leading to a low survival rate [2, 3]. Aberrant glycan structures have been shown to be universal characteristics of malignancies and to regulate the development and progression of cancers [4–6]; they can serve as clinical biomarkers and provide specific targets for therapeutic intervention [5, 7]. Common alterations of glycosylation in cancer include elevations in truncated *O*-glycans and highly branched complex *N*-glycans, as well as modifications in the expression of fucosylated and sialylated glycans that were found to be related to tumorigenesis [8, 9]. These aberrant glycosylation patterns could result from changes in the corresponding glycosyltransferase activities and the availability of enzyme substrates [10].

A key feature of metastasized cancer cells is the requirement of adhesive interactions. Many of these are mediated through the recognition of sialic acid containing glycans such as sialyl-Lewis^x, sialyl-Tn and sialyl-3T antigens that also provide favorable conditions for tumor dissemination [11–15]. The sialyl-3T antigen (Neu5Ac α 2-3Gal β 1-3GalNAc-) synthesized by α 2,3-sialyltransferase-I (ST3Gal-I) was shown to be upregulated in breast [16], ovarian [17], brain [18] and renal cancers [19] with worse prognosis and reduced overall survival [20–22]. In

Ruifeng Bai and Xue Luan contributed equally to this work

Electronic supplementary material The online version of this article (<https://doi.org/10.1007/s10719-020-09927-x>) contains supplementary material, which is available to authorized users.

✉ Yin Gao
yin.gao@queensu.ca

¹ Key Laboratory for Molecular Enzymology and Engineering of Ministry of Education, School of Life Sciences, Jilin University, 130012 Changchun, China

² Univ. Lille, CNRS, UMR8576 – UGSF – Unité de Glycobiologie Structurale et Fonctionnelle, F-59000 Lille, France

³ Department of Biomedical and Molecular Sciences, Queen's University, Kingston, ON, Canada

contrast, reduced expression of ST3Gal-I was detected in lung cancer [14]. ST3Gal-I was also found to be related to anti-cancer drug resistance [17, 23]. Down regulation of ST3Gal-I reduced tumor growth, migration, invasion and angiogenesis in ovarian and breast cancers *in vitro*, in cell cultures and in cancer cell xenograft tumor model of mice [17, 20, 21]. However, the pathological role of ST3Gal-I in prostate cancer progression still needs to be elucidated.

We previously determined the expression levels and activities of glycosyltransferases in cultured CaP cells, and proposed the glycosylation pathways in CaP, compared to normal prostate cells [24]. The results showed that all CaP cells were able to synthesize core 1. The androgen dependent CaP cells (LNCaP and VCaP) showed higher core 2 synthase activity, whereas androgen independent CaP cells (PC-3 and DU145) showed undetectable core 2 synthase activity. Thus in PC-3 and DU145 cells simple short *O*-glycans are expected to be abundant. Moreover, the activity and expression levels of ST3Gal-I were dramatically increased in PC-3 cells, which can lead to the increased production of sialyl-3T antigen. Herein, we describe a comprehensive study of *O*-glycosylation patterns of metastatic CaP cell lines (PC-3 derived from bone metastasis, LNCaP derived from lymph node metastasis, VCaP derived from vertebra metastasis, and DU145 derived from brain metastasis) and a transformed cell line from normal prostate (RWPE-1) via Matrix-assisted laser desorption/ionization-time of flight mass spectrometry (MALDI-TOF-MS) analysis. Consistent with previous studies, the sialyl-3T antigen was found especially abundant in PC-3 cells. We therefore investigated the role of ST3Gal-I in cultured PC-3 cells and in a xenograft mouse model. Our collective results showed a correlation of ST3Gal-I with PC-3 cell proliferation, migration and apoptosis in cell cultures, as well as with solid tumor formation in xenograft mouse model. This study helps to identify a prognosis biomarker and therapeutic target for prostate cancer treatment.

Materials and methods

Cell cultures

The immortalized human prostate cell line RWPE-1 was purchased from ATCC and grown in keratinocyte serum-free medium with growth kit (Invitrogen). All CaP cell lines (PC-3, LNCaP, VCaP, DU145) were obtained from ATCC and were grown as previously described [24]. Reagents were purchased from Sigma unless stated otherwise.

Glycoprotein sample preparation

Cells collected from cultures of each prostate cell line were homogenized and delipidated as described [25]. Briefly, cellular lipids were extracted with chloroform/methanol (2:1, v/v).

Insoluble proteins were collected by centrifugation, washed with cold-acetone/water (4:1, v/v) and dried under N₂ followed by lyophilizing. The obtained protein samples were resuspended in 0.1 M Tris/HCl, pH 8 containing 6 M guanidinium chloride and 5 mM ethylenediaminetetraacetic acid. Dithiothreitol was then added to a final concentration of 20 mM and the mixture was incubated at 37 °C for 1 h. After 1 h incubation iodoacetamide was added to a final concentration of 50 mM, followed by an overnight incubation at room temperature in the dark. This alkylated protein sample was dialyzed against deionized water at 4 °C for three days with changing of water every 24 h. Samples were then freeze-dried after dialysis. Denatured protein samples were digested with trypsin overnight at 37 °C. After trypsinization, protein samples were boiled for 5 min to inactivate all trypsin enzyme activities and then centrifuged at 100 × g for 30 min. The supernatants were collected and dried. Salts and free sugars in samples were removed by a C18 Sep-Pak cartridge (Solid phase extraction high capacity, Grace). Peptides and glycopeptides were eluted with a step gradient of 20, 40 and 60% isopropanol in 5% acetic acid. Eluents were dried under N₂ followed by freeze drying. The lyophilized proteins were dissolved in 200 µL of freshly prepared 50 mM ammonium hydrogen carbonate solution. PNGase F enzyme solution (3 µL, 1000U/mL, Roche) was added to each sample followed by the incubation at 37 °C overnight to release N-glycans. After digestion, samples were loaded onto C18 Sep-Pak cartridges and washed with 16 mL 5% acetic acid. The fractions of flow through and the wash were the *N*-glycan containing fractions. Peptides and *O*-glycopeptides were eluted with a gradient of 20, 40, and 60% isopropanol in 5% acetic acid and dried under nitrogen followed by lyophilization and were subjected to reductive elimination.

O-glycan Preparation

Lyophilized proteins were dissolved in 200 µL of freshly prepared 50 mM ammonium hydrogen carbonate solution. *O*-glycans were released by β-elimination reaction with freshly prepared 100 mM NaOH containing 1 M NaBH₄. The reaction was carried out at 45 °C overnight, then stopped by addition of 10% acetic acid. The released *O*-glycans were desalted with Dowex 50WX8, hydrogen form. Borate in the samples was removed with methanol evaporation. Samples were further purified through a graphitic column (Carboglyph 1SPE 120/400 Mesh, Grace), washed with 10 mL 0.1% trifluoro acetic acid (TFA). Sequential elution was achieved with 25, 50 and 80% acetonitrile in 0.1% TFA. The eluted fractions were dried under nitrogen and then lyophilized overnight.

Preparation of permethylated O-glycans

Vials containing the freeze-dried glycan samples were kept in a desiccator under an argon atmosphere. DMSO (400 µL) was

added into each vial to dissolve glycans; then 25 mg powdered NaOH and 300 μ L ICH_3 were added in sequence. Mixtures were flushed with a stream of argon, and tubes were capped and sealed. After vortexing the mixture at room temperature for 30 min, the reaction was quenched by adding 1 mL 5% acetic acid. Permethylated glycans were extracted by the addition of 1 mL of chloroform. After mixing vigorously, the chloroform layer was transferred into a clean tube and washed 3 times with 1 mL of water at 4 °C. The chloroform layer was transferred into a glass tube and dried under a stream of nitrogen in the hood and then freeze dried. Permethylated glycans were further purified with Sep-Pak C18 columns which were washed with 7 mL water and 2 mL 10% acetonitrile. The permethylated glycans were eluted with 2 mL 80% acetonitrile. Eluates were collected and the acetonitrile content was evaporated under a stream of N_2 followed by lyophilization.

Preparation of permethylated glycans for MALDI-TOF-MS

Permethylated glycans were dissolved in 30 μ L methanol/water (1:1, v/v) then mixed at a 1:1 ratio with matrix 2,5-dihydroxybenzoic acid. The sample mixture (0.5–1.0 μ L) was loaded directly onto the MALDI target plate. The mixture was allowed to dry at room temperature.

Acquisition of MALDI-TOF-MS spectra

The procedure of acquiring the spectra was carried out as published [26, 27]. Spectra were obtained by submitting each spot to pulsed nitrogen laser shots over a range of m/z ratio from 400 to 2000 for permethylated *O*-glycans. The laser spot was moved to different areas of the target during acquisition, and spectra were averaged until a satisfactory signal-to-noise ratio was obtained.

Small interference RNA (siRNA) transfection

PC-3 cells were transfected with either ST3Gal-I siRNA or siRNA with a nonsense/scrambled sequence (as a negative control) by using Lipofectamine®2000 Transfection reagent (Invitrogen) according to the manufacturing instructions. The designed oligonucleotides of the ST3Gal-I siRNA were 5'-UGAACCUUCUCAUCGAACCAATT-3', 5'-UGGUUCGAUGAGAGGUUCATT-3'. The nonsense siRNA were 5'-UUCUCCGAACGUGUCACGUTT-3' and 5'-ACGUGACACGUUCGGAGAATT-3' (GenePharma). The cellular uptake efficiency was determined via flow cytometry after transfecting PC-3 cells with FAM-labeled siRNA (GenePharma).

Western blots

Proteins prepared from cell lysates were separated by SDS-PAGE, then transferred to PVDF membranes. Membranes were first incubated with primary antibody followed by the incubation with a secondary antibody according to the manufacturing instructions. Mouse monoclonal anti-ST3GalT-I antibody as the primary antibody (Sigma) and horseradish peroxidase-conjugated goat anti-mouse IgG as the secondary antibody (Abcam) were used to determine the level of ST3Gal-I in PC-3 cells. Human glyceraldehyde-3-phosphate dehydrogenase (Abcam) was used as a control.

Cell proliferation

MTT (3-(4,5-dimethylthiazol-2-yl)-2,5-diphenyltetrazolium bromide) assays were utilized to evaluate the growth inhibitory effect imposed by down regulating the expression of ST3Gal-I in PC-3 cells. After 24 h transfection, cell growth medium was replaced and cells were incubated for 1 to 4 days. At the end of the incubation time, medium was removed followed by the addition of 200 μ L of 5 mg/mL MTT in Phosphate buffered saline (PBS). After 4 h of incubation, the supernatant was removed and washed, and DMSO was then added to each well under gentle agitation for 10 min until complete dissolution was achieved. A negative control group consisting of cells that were not subjected to siRNA transfection was normalized as 100% for the cell growth. The spectrophotometric absorbance of the samples was measured using a micro-titer plate reader at a wavelength of 490 nm.

Cell migration

Scratched wound healing and transwell assays were performed to assess the migration ability of PC-3 cells after siRNA transfection. For scratched wound healing assays, PC-3 cells were seeded in 6-well plates at a density of 4×10^5 cells per well and incubated until 100% confluency was reached. The scratches were made by pipette tips through the monolayer in the middle of the plate. Cells were washed and then incubated for 24 to 48 h. Images were taken using a microscope (Olympus). For transwell assays, PC-3 cells were seeded in the inserts of a 24-well plate. Serum free medium (100 μ L) was added to the insert and 600 μ L 10% FBS serum medium were added to the lower chamber of a 24-well plate as a chemoattractant. After 48 h incubation, non-migrating cells were removed by wiping the upper side of the insert with a cotton swab. Migrated cells on the bottom side of the insert were quantified using a microscope.

Lectin staining

Lectin staining assay was performed to assess the cell surface glycosylation via a previously reported method [24]. Briefly, after transfection or treatment with 1 and 5 mU/mL α 2–3,6 neuraminidase for 1, 3 and 24 h, cells were subjected to lectin staining analysis. Lectin staining was performed on cells that were fixed in 96-well microtiter plates and incubated with biotinylated lectins: *Ricinus communis* agglutinin I (RCA, Vector) that recognizes Gal, *Maackia amurensis* Lectin II (MAL II, Vector) that recognizes Neu5Ac(α 2–3), *Sambucus nigra* lectin (SNA, Vector) that recognizes Neu5Ac(α 2–6), Peanut agglutinin (PNA, Vector) that recognizes Gal-GalNAc (core 1 structure), Concanavalin A (ConA, Vector) that recognizes mannose and Wheat germ agglutinin (WGA, Vector) that recognizes GlcNAc. This was followed by incubation with alkaline phosphatase-conjugated avidin and nitrophenyl-phosphate reaction substrate. The absorbance was measured with a microplate reader at 405 nm.

T-antigen expression

The expression of T-antigen in PC-3 cells was assessed after nonsense siRNA or ST3Gal-I siRNA transfection with mouse monoclonal anti-Thomsen-Friedenreich antigen antibody (Abnova, China) and the goat anti-mouse FITC-conjugated secondary antibody according to the manufacturer's instructions. The immunofluorescent staining on cell surfaces was detected via flow cytometry.

Cell apoptosis

PC-3 cells either transfected or treated with 5 mUnit/ml of α 2–3,6 neuraminidase for 24 h were induced with human TRAIL (2 ng/mL, Cedarlane) for an additional 48 to 72 h. Cells were then stained using the Annexin V-FITC Apoptosis Kit (Absin) and subjected to flow cytometry analysis. Briefly, cells (1.5×10^5) from each time point were resuspended into FACS Buffer (PBS, 1% BSA, 0.1% NaN_3) and kept in the dark. The fluorescence was detected via flow cytometry.

The expression of death receptor DR4 and DR5 in PC-3 cells was assessed after siRNA transfection with FITC conjugated mouse monoclonal anti-DR4/5 antibody (Abcam) according to the manufacturer's instructions. The immunofluorescent staining on cell surfaces was detected by flow cytometry.

In vivo xenograft mouse model

Male Balb/c nude mice, 6–8 weeks old, weighing 18–20 g each were purchased from the Liaoning Changsheng

Biotechnology Company Ltd, China. These mice were housed in plastic cages and maintained on a 12 h light/dark cycle (lights on 7:00–19:00 h) under standard laboratory conditions of 55% relative humidity and at 23 ± 1 °C. They were given standard chow (Liaoning Changsheng Biotechnology Company Ltd, China) and tap water *ad libitum*. Prior to the experiments, the entire animal protocol was reviewed and approved by the Institution Animal Ethics Committee (Reference No. SY201905023), and adhered to the Guidelines on Humane Treatment to Lab Animals (2009) [28]. Nude mice were randomly divided into three groups ($n = 05$ per group): the untransfected, ST3Gal-I siRNA and the nonsense siRNA transfected groups. To establish the xenograft mouse model, PC-3 cell suspension ($100 \mu\text{L}$, 10^7 cells) was subcutaneously inoculated into the armpit of nude mice. The volumes of tumors and body weight of the nude mice were measured at fixed intervals after 2 weeks from the day of implantation.

Results

O-glycan profiles of human prostate cells

O-linked glycans from normal and prostate cancer cell lines were analyzed and the proposed monosaccharide compositions were compared in Table 1. Common core structures 1 ($\text{Gal}\beta 1\text{-3GalNAc}$) and 2 ($\text{Gal}\beta 1\text{-3(GlcNAc}\beta 1\text{-6)GalNAc}$) and possibly also core 3 ($\text{GlcNAc}\beta 1\text{-3GalNAc}$) and core 4 ($\text{GlcNAc}\beta 1\text{-3(GlcNAc}\beta 1\text{-6)GalNAc}$) were found in all cell types. Even if only one single sample for each cell line was investigated, this semi-quantitative analysis via MS seems to indicate an increased expression of simple/short O-glycans in PC-3, DU145 and VCaP cells (Fig. 1A), with higher amounts in the androgen-independent CaP cells (PC-3 and DU145) than the androgen-dependent CaP (VCaP). LNCaP and RWPE-1 cells showed similar levels of simple/short O-glycans (Fig. 1A).

Complex O-glycans were detected at lower levels in PC-3, DU145 and VCaP cells, compared to the normal RWPE-1 cells, with PC-3 and DU145 cells showing less of the complex O-glycans than LNCaP and VCaP cells. Moreover, the level of O-glycan fucosylation was decreased in all CaP cells, while the sialylation of O-glycan was elevated in CaP cells compared to RWPE-1 cells (Fig. 1B). Based on this semi-quantitative analysis, the calculated proportion of sialyl-T antigen among O-glycans in normal RWPE-1 prostate cells was lower than all CaP cells (Fig. 1C). Moreover, the androgen-independent cells PC-3 exhibited the highest sialyl-3T and disialyl-T among these CaP cells (Fig. 1C; Table 1). Mass spectrometry data of O-glycan analysis was exported and shown in the Supplementary Information as Table S1 and

Figure S1. The spectra of isotopic envelope match with the expected theoretical mass as shown in the Supplementary Information (Figure S2). The available MS/MS data are listed in the Supplementary Information (Figure S3).

Among these short *O*-glycans, the sialyl-T antigen, Neu5Ac α 2-3Gal β 1-3GalNAc-ol (m/z 895.5, the fragmentation spectrum is shown in Figure S3) and di-sialyl-T antigen (m/z 1256.6, the fragmentation spectrum is shown in Figure S3) appeared to be abundant in all CaP cells (Figure S1, S3). Especially in PC-3 cells (Figure S1B, Table 1), the presence of sialyl-3T antigen was highest among the CaP cell lines. The MS/MS data of m/z 895.5 indicated that it was sialyl-T antigen (fragments: m/z 620.2, NeuAc-Gal-), as there were no fragments of sialyl-6T (m/z 659.3, NeuAc-GalNAc-) present in the spectrum (Figure S3). We therefore focused on exploring the possible function of sialyl-3T antigens and ST3Gal-I in PC-3 cells and in the xenograft mice experiments.

ST3Gal-I knockdown suppresses PC-3 cell proliferation and migration

To unravel the role of ST3Gal-I in metastatic CaP cells, PC-3 cells that highly express sialyl-3T were selected to perform ST3Gal-I silencing via ST3Gal-I siRNA. In comparison to the untransfected and nonsense siRNA transfected PC-3 cells, ST3Gal-I expression in ST3Gal-I siRNA transfected cells was significantly reduced after 48 h (Fig. 2A). Uptake efficiency was evaluated using FAM-labeled siRNA transfection (Fig. 2B). The lectin staining analysis showed that the level of α 2,6 linked sialic acid and GlcNAc, recognized by SNA and WGA, remained unchanged after 48 h post transfection. However, there was decreased MAL II binding and increased PNA binding to ST3Gal-I siRNA transfected cells, indicating that less α 2,3 linked sialic acid and more core 1 structures were present on cell surfaces due to the down regulation of ST3Gal-I (Fig. 2C). The binding of T-antigen antibody to cell surfaces was increased significantly after ST3Gal-I siRNA transfection in comparison to the nonsense siRNA transfected cells. This indicated that there were more T-antigen structures exposed, due to the knockdown of ST3Gal-I and the decreased levels of sialyl-3T (Fig. 2D).

MTT assays performed after 24 to 96 h transfection indicated that down regulation of ST3Gal-I expression inhibited PC-3 cell growth (Fig. 2E). Moreover, knockdown of ST3Gal-I in PC-3 cells significantly decreased the number of migrating cells, and resulted as larger wound areas when compared with the nonsense siRNA transfected cells (Fig. 3A). To further confirm the observation in scratched wound healing assays, transwell migration assays were performed where cells were grown after 24 h transfection for another 48 h to allow migration (Figure S4). The results showed that

in vitro cell migration was remarkably inhibited after down-regulation of ST3Gal-I (Fig. 3B).

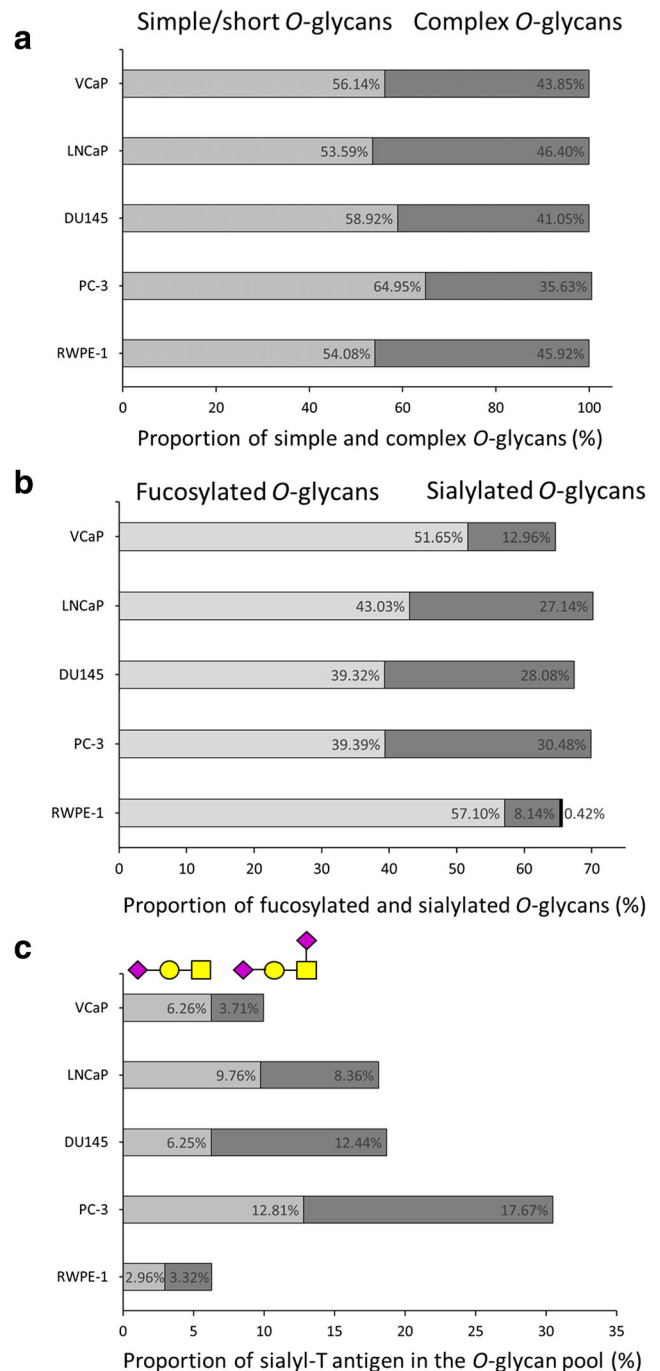


Fig. 1 Glycosylation pattern analysis based on the MALDI-TOF mass spectrometry. **A** The proportions of simple and complex *O*-glycans; light gray, simple *O*-glycan; dark gray, complex *O*-glycan in the *O*-glycan pool. **B** The proportions of fucosylated and sialylated *O*-glycans in the *O*-glycan pool, light gray, fucosylated *O*-glycan; dark gray, sialylated *O*-glycan; black, glycan decorated with both and fucosylation and sialylation. **C** Proportion of sialyl-T antigen in the *O*-glycan pool; light gray, sialyl-3T, dark gray, di-sialyl-T

ST3Gal-I knockdown increases the sensitivity of PC-3 cells to TRAIL

Death receptors DR4 and 5 are *O*-glycosylated, and *O*-glycosylation was shown to facilitate tumor necrosis factor-related apoptosis inducing ligand (TRAIL) induced clustering of DR4 and DR5 [29]. We therefore evaluated TRAIL induced apoptosis by cells transfected with ST3Gal-I and nonsense siRNA. The levels of early and late apoptosis were determined

via the Annexin V-FITC kit in conjunction with propidium iodide (PI) staining, followed by flow cytometry analysis. As shown in Fig. 4, apoptosis was detected after treatment of cells with TRAIL (2 ng/mL) for 48 and 72 h. Down regulation of ST3Gal-I increased the sensitivity of PC-3 cells to TRAIL induced apoptosis. These results were further confirmed after treatment of PC-3 cells with 5 mU/mL α 2–3,6-neuraminidase for 3 h. The efficiency of neuraminidase treatment was shown with lectin binding assays (Figure S5). A substantial reduction

Table 1 Deduced monosaccharide compositions and the relative intensity of the major *O*-glycans from cultured human prostate control cells (RWPE-1) and prostate cancer cells (PC-3, DU145, LNCaP, VCaP) obtained from MALDI-TOF mass spectrometry. *O*-glycans were released by β -elimination and then permethylated prior to analysis

<i>O</i> -linked glycan composition	Expected <i>m/z</i>	Relative Intensity (%)				
		RWPE-1	PC-3	DU145	LNCaP	VCaP
Gal1Fuc1GalNAcol + 1Na	708.38	5.0	4.0	4.8	4.0	5.6
Gal1GlcNAc1GalNAcol + 1Na	779.41	8.0	7.9	8.4	7.0	8.9
Gal1NeuAc1GalNAcol + 1Na	895.46	3.0	12.8	6.2	9.8	6.3
Gal1GlcNAc1Fuc1GalNAcol + 1Na	953.50	6.1	4.3	5.8	3.9	6.0
Gal2GlcNAc1GalNAcol + 1Na	983.51	3.0	1.8	5.7	4.0	3.0
Gal1GlcNAc2GalNAcol + 1Na	1024.54	6.4	4.1	3.2	4.1	4.8
Gal1NeuAc1Fuc1GalNAcol + 1Na	1069.55	0.4	/	/	/	/
Gal1GlcNAc1Fuc2GalNAcol + 1H	1105.61	/	/	/	/	0.9
Gal1GlcNAc1NeuAc1GalNAcol + 1Na	1140.59	0.9	/	0.6	1.0	0.8
Gal2GlcNAc1Fuc1GalNAcol + 1Na	1157.60	6.7	3.9	3.8	4.6	6.2
Gal1GlcNAc2Fuc1GalNAcol + 1Na	1198.63	3.1	2.1	2.0	1.7	2.5
Gal2GlcNAc2GalNAcol + 1Na	1228.64	4.8	4.2	4.2	3.1	5.3
Gal1NeuAc2GalNAcol + 1Na	1256.64	3.3	17.7	12.4	8.4	3.7
Gal1GlcNAc3GalNAcol + 1Na	1269.67	3.3	2.2	1.7	2.0	2.2
Gal2GlcNAc1Fuc2GalNAcol + 1Na	1331.69	11.0	7.3	5.5	6.4	7.9
Gal2GlcNAc1NeuAc1GalNAcol + 1Na	1344.69	0.9	/	8.2	8.1	2.1
Gal2GlcNAc2Fuc1GalNAcol + 1Na	1402.73	12.1	9.9	7.7	9.2	9.9
Gal3GlcNAc2GalNAcol + 1Na	1432.74	1.0	0.9	0.9	0.7	0.9
Gal2GlcNAc3GalNAcol + 1Na	1473.77	7.0	8.6	7.9	8.0	8.9
Gal2GlcNAc2Fuc2GalNAcol + 1Na	1576.82	1.9	1.1	1.4	1.0	1.6
Gal1GlcNAc3Fuc2GalNAcol + 1H	1595.86	/	0.8	0.9	2.1	2.7
Gal3GlcNAc2Fuc1GalNAcol + 1Na	1606.83	1.0	/	0.9	0.7	1.0
Gal1GlcNAc3Fuc2GalNAcol + 1Na	1617.85	/	/	0.9	/	/
Gal2GlcNAc3Fuc1GalNAcol + 1Na	1647.86	4.8	3.0	3.4	4.4	3.4
Gal3GlcNAc3GalNAcol + 1Na	1677.87	0.4	0.6	/	0.5	0.6
Gal3GlcNAc2Fuc2GalNAcol + 1Na	1780.92	1.5	0.7	0.6	0.9	/
Gal2GlcNAc3Fuc2GalNAcol + 1H	1799.96	/	0.9	1.2	1.6	1.8
Gal2GlcNAc3Fuc2GalNAcol + 1Na	1821.95	1.0	/	0.5	0.6	/
Gal3GlcNAc3Fuc1GalNAcol + 1Na	1851.96	0.7	0.8	/	0.7	0.9
Gal3GlcNAc4GalNAcol + 1Na	1922.99	0.3	/	0.5	/	0.6
Gal3GlcNAc3Fuc2GalNAcol + 1H	2004.06	/	0.6	/	/	0.7
Gal3GlcNAc3Fuc2GalNAcol + 1Na	2026.05	0.8	/	/	/	0.6
Gal4GlcNAc3Fuc1GalNAcol + 1Na	2056.06	0.2	/	/	0.3	/
Gal3GlcNAc4Fuc1GalNAcol + 1Na	2097.08	0.4	/	/	0.5	/
Gal3GlcNAc2NeuAc2GalNAcol + 1Na	2155.09	/	/	0.6	/	/
Gal3GlcNAc5GalNAcol + 1Na	2168.12	0.2	/	/	0.3	0.3
Gal4GlcNAc3Fuc2GalNAcol + 1Na	2230.15	0.2	/	/	0.3	/
Gal4GlcNAc3Fuc3GalNAcol + 1Na	2404.23	0.4	/	/	0.2	/

of $\alpha 2,3$ linked sialic acid structures was achieved while the level of $\alpha 2,6$ linked sialic acids remained constant. As expected, the binding of RCA (recognizing Gal) was increased due to the reduction of sialyl $\alpha 2-3$ Gal linkages. The removal of $\alpha 2-3,6$ linked sialic acids from cell surfaces rendered PC-3 cells more susceptible to TRAIL, suggesting that the high expression of ST3Gal-I and sialic acids prevented apoptosis induced by TRAIL. The expression levels of DR4 and 5 in PC-3 cells, measured by flow cytometry, remained unchanged after 24 and 48 h ST3Gal-I siRNA transfection (Figure S6). Therefore, the increased susceptibility of PC-3 cells to apoptosis after down regulation of ST3Gal-I was associated with

the reduced level of sialyl-3T, rather than an increased expression of death receptors in transfected cells.

ST3Gal-I silencing suppresses the tumorigenicity of PC-3 cells in BALB/c nude mice

To investigate the relationship between ST3Gal-I and tumorigenesis, PC-3 cells were transfected with either nonsense or ST3Gal-I siRNA and then subcutaneously injected into athymic nude mice. As shown in Fig. 5A, down regulation of ST3Gal-I reduced the growth of PC-3 *in vivo* and resulted in

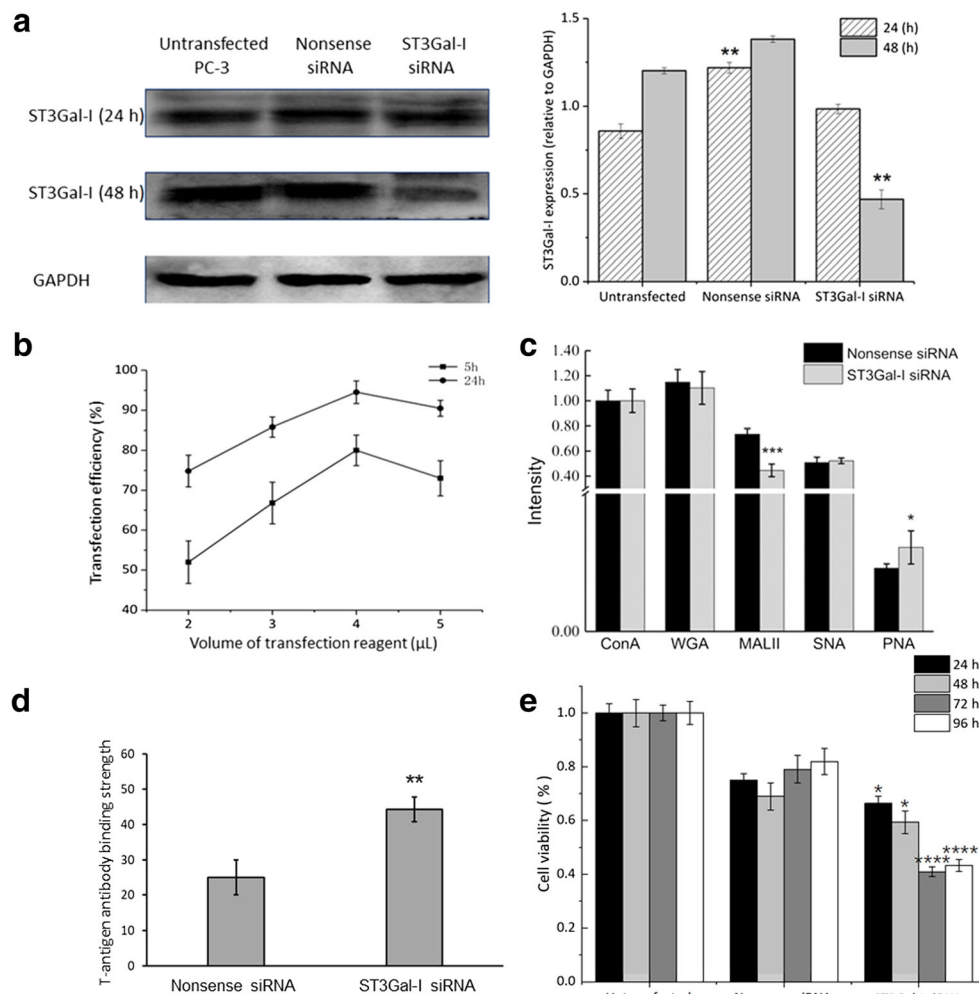
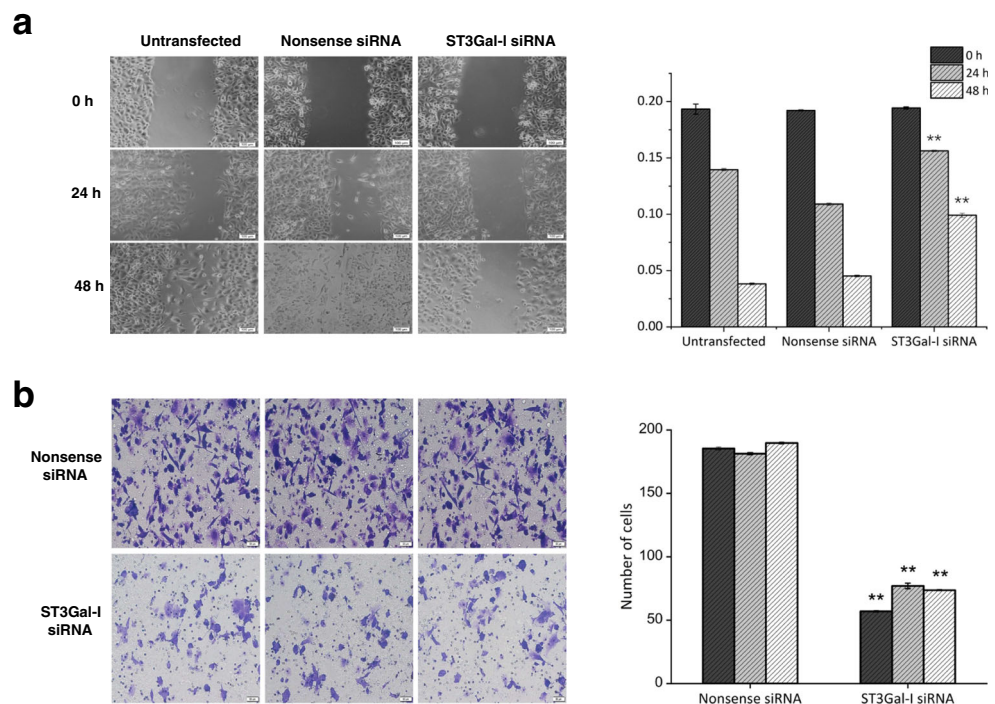


Fig. 2 Down-regulation of ST3Gal-I reduces PC-3 cell proliferation *in vitro*. **A** Determination of ST3Gal-I expression in PC-3 cells transfected with nonsense and ST3Gal-I siRNA by western blot. Data represent the mean \pm SD of the expression levels standardized to GAPDH expression. Data shown are the mean \pm SD of three separate experiments (* p < 0.05, ** p < 0.01, compared to untransfected group). **B** Transfection efficiency was assessed with FAM-conjugated siRNA, and 4 μ L transfection reagents plus 24 h transfection time provided the optimal transfection condition. Data shown are the mean \pm SD of three separate experiments. **C** Lectin staining of PC-3 cells after transfection

with nonsense and ST3Gal-I siRNA. Data shown are the mean \pm SD of six separate experiments (* p < 0.05, *** p < 0.001, compared to nonsense siRNA transfection group). **D** T-antigen binding strength of PC-3 cells after transfection with nonsense and ST3Gal-I siRNA. Data shown are the mean \pm SD of three separate experiments (** p < 0.01, compared to nonsense siRNA transfection group). **E** Proliferation of PC-3 cells following ST3Gal-I siRNA transfection was evaluated by MTT assay at 24 to 96 h, and the cell viability (%) of PC-3. Data shown are the mean \pm SD of seven separate experiments (* p < 0.05, **** p < 0.0001, compared to nonsense siRNA groups)

Fig. 3 Down-regulation of ST3Gal-I reduces migration of PC-3 cells *in vitro*. **A** The migration abilities of PC-3 with down regulated expression level of ST3Gal-I were determined by wound healing assay at 24 and 48 h. Area, the cell free areas (wounds). Data represent the mean \pm SD of three independent experiments (** $p < 0.01$, compared to nonsense siRNA transfection group). **B** Transwell migration of PC-3 cells with ST3Gal-I knocked-down was assayed at 48 h. Total numbers of cells in seven random fields were counted. Data shown are the mean \pm SD of three separate experiments (** $p < 0.01$, compared to nonsense siRNA transfection group)



drastically reduced volume of engrafted tumors in mice. The proteins extracted from the tumor tissues were also analyzed by western blot to compare the expression levels of ST3Gal-I and death receptors DR4 and 5. As shown in Fig. 5B, the expression of DR4 and 5 remained unchanged, while the ST3Gal-I levels were lower in the engrafted tumor that formed from ST3Gal-I siRNA transfected PC-3 cells. In this experiment, the body

weight of mice after xenotransplantation remained similar for the entire experimental period (Figure S7).

Discussion

In the present study, the total cellular glycoprotein derived *O*-glycan patterns of cultured human CaP cells (PC-3, DU145, LNCaP, and VCaP) were analyzed by MALDI-TOF MS in comparison to normal prostate cells (RWPE-1). Based on the descriptions in the Materials and method section, the *N*-glycans were removed using PNGase F from the same glycopeptide preparation prior to *O*-glycan removal using beta-elimination, and there was no evidence of *N*-glycans present according to MS spectra (Figure S1). Clearly, there is a diversity of *O*-glycan patterns among these cell lines, and this may echo the diversity among different human prostate tumors. The prostate cancer cell lines studied here were derived from different metastatic sites with different biological properties but nevertheless showed some similarities in their glycan patterns. The question remains how many features of the original tumor remain in the cultured CaP model cells and what the functional significance of this heterogeneity is.

MS is a sensitive method but fails to define the exact linkages between sugars and often cannot distinguish between isomeric structures. However, MS-MS fragmentation is useful to distinguish between isomers. Our MS analysis suggested that simple short *O*-glycans were highly expressed in androgen-independent CaP cells (PC-3 and DU145)

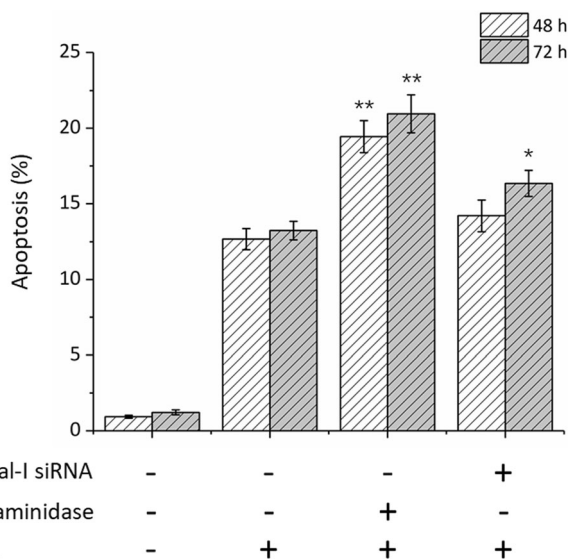


Fig. 4 TRAIL-induced apoptosis in PC-3 cells. PC-3 cells were subjected to TRAIL (2 ng/mL) induction after ST3Gal-I-silencing or after the α 2-3,6-neuraminidase treatment. Data shown are the mean \pm SD of three separate experiments (* $p < 0.05$, ** $p < 0.01$, compared to TRAIL alone groups)

compared to androgen-dependent CaP cells (VCAp). The predominant *O*-glycans from prostate cancer cells had relatively simple structures (Fig. 1), e.g. the sialylated core 1 structure, determined to be sialyl-3T via MS/MS analysis. The polypeptide GalNAc-transferase and core 1 synthase that synthesize core 1 *O*-glycans are active in all prostatic cells [24]. It is possible that additional core structures are present at low levels such as core 2, 3 and 4 structures. However, only RWPE-1 cells, LNCaP and VCap, but not PC-3 and DU145 cells, have the activity to synthesize the branched core 2 structure, as indicated in our previous studies [24]. MS analysis showed that complex *O*-glycans were detected at a lower level in all CaP cells compared to the normal RWPE-1 cells. Although the core 2 structures are minor components of the total *O*-glycans in CaP cells, core 2 β 1,6-GlcNAc-transferase was shown to be involved in prostate cancer progression [30] and to associate with prostate cancer aggressiveness [31]. The GlcNAc-transferase activity that synthesizes core 3 was only detected in RWPE-1 cells and no core 4 GlcNAc-transferase activity was detected in any of the prostatic cells [24]. It is possible that at a low level of enzyme expression and undetectable activity cells synthesize a small amount of these additional *O*-glycans that can be measured by the sensitive MS method.

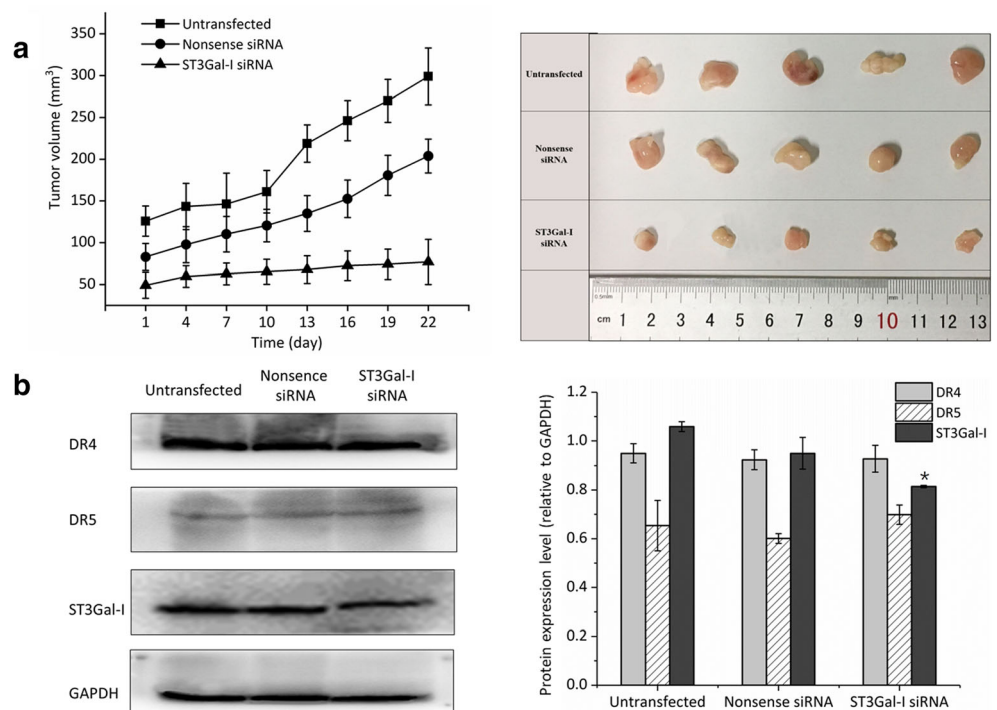
The mono-sialylated core 1 structures (sialyl-T antigens, *m/z* 895.8) are especially abundant in the cancer cells (Figure S1, S3). This is consistent with CaP having relatively high sialyltransferase activities [24]. However, since the MS analysis was done with single sample, we cannot conclude

that sialyl-T antigens were elevated with statistical significance. We previously showed that in PC-3 and LNCaP cells, the activities as well as the mRNA expression of ST3Gal-I, were increased. A high expression of sialyl-3T has also been found in other cancer cells, including mammary and gastric carcinoma cells [15, 32]. ST3Gal-I is the major enzyme that transfers sialic acid to core 1 to synthesize the sialyl-3T antigen [10]. We therefore focused on exploring the possible function of sialyl-T antigens and ST3Gal-I in the metastatic process.

Cancer cells exhibit characteristics such as unlimited proliferation and decreased apoptosis, and abnormal ability to migrate. Many of the cell surface receptors involved in regulating cell growth and proliferation are glycoproteins but the glycan functions have received minimal attention. The TNF superfamily of death receptors (TNFR), including DR4, DR5 and Fas (CD95), carry glycans with potential roles in ligand binding and receptor oligomerization which leads to downstream apoptotic signaling events [23]. This study showed that down regulation of ST3Gal-I through siRNA interference resulted in an inhibition of PC-3 cell proliferation (Fig. 2). The branching and elongation of core 1 is blocked by sialylation [10, 33]. Core 1 sialylation by overexpressing ST3Gal-I reduced the number of terminal Gal residues and rendered prostate cancer cells resistant to galectin-1 induced apoptosis. This suggests that the sialyl-3T antigen is critical for cancer cells to evade the immune system [34].

Both *N*- and *O*-glycans appear to be important in TRAIL-induced apoptosis. Excessive *O*-glycosylation achieved by

Fig. 5 Down-regulation of ST3Gal-I reduces PC-3 cell proliferation and tumor growth *in vivo*. Tumors formed in the untransfected, nonsense siRNA transfected and ST3Gal-I transfected PC-3 implanted mice are shown. **A** Comparison of tumor volume. Tumors formed from ST3Gal-I siRNA transfected PC-3 cells exhibited the smallest volume than the untransfected and nonsense siRNA transfected groups. Data shown are the mean \pm SD of three separate measurements. **(B)** Proteins extracted from tumor tissues were analyzed by western blot. The band density was analyzed with Image J. Data represent the mean \pm SD of the expression levels standardized to GAPDH expression (* $p < 0.05$, compared to nonsense siRNA transfection group)



overexpression of ppGalNAcT14 increased the sensitivity to TRAIL-induced apoptosis through DR4 and DR5 [29]. In addition, inhibition of *N*-glycan synthesis by tunicamycin led to an up-regulation of DR5 which consequently enhanced the sensitivity to TRAIL-induced apoptosis in prostate cancer cells [35]. Our studies showed that down regulation of ST3Gal-I in PC-3 cells led to a minor increase in susceptibility to TRAIL-induced apoptosis but had no effect on the receptor expression (Fig. 4). This suggests that the high expression of ST3Gal-I in CaP cells contributes to the resistance to apoptosis by preventing ligand-receptor interactions. A suggested mechanism for receptor function is that negatively charged sialic acid residues prevent co-clustering of DR4/5 in lipid rafts. Therefore, decreased sialylation may facilitate TRAIL-induced apoptosis. This is consistent with our observation that ST3Gal-I contributes to CaP tumor growth in the xenograft mouse model in which the downregulation of ST3Gal-I results in much smaller tumor sizes (Fig. 5A). The western blot analysis indicated that the expression of DR4 and 5 remained unchanged, while the ST3Gal-I levels were lower in the engrafted tumor that formed from ST3Gal-I siRNA transfected PC-3 cells (Fig. 5B). This suggested that the ST3Gal-I promoted the growth of tumor *in vivo*. In addition, our results suggest that ST3Gal-I has a critical role in CaP cell invasion and metastasis; it promotes PC-3 cell migration which is significantly reduced by down regulation of ST3Gal-I (Fig. 3). A similar observation was made in a study of breast cancer where sialylated core 1 and overexpression of ST3Gal-I supported mammary tumorigenesis [36, 37]. Overexpression of ST3Gal-I also promoted migration and invasion of hepatocellular carcinoma cells [38].

Our comprehensive study of *O*-glycomics and glycan functions of prostatic cell lines has important implications. It defines sialyl-3T and ST3Gal-I as potential therapeutic targets and a basis for anti-cancer drug development.

Funding information This work was supported by the National Natural Science Foundation of China [31700713]; Department of Science and Technology of Jilin Province [grant number 20200801066GH]; Jilin Province Development and Reform Commission [2019C049-9] to Y.G. and Prostate Cancer Fight Foundation, Canada to I.B.

Compliance with ethical standards

Conflict of interest The authors declare that they have no conflicts of interest.

Ethical approval Prior to the experiments, the entire animal protocol was reviewed and approved by the Institution Animal Ethics Committee (Reference No. SY201905023), and adhered to the Guidelines on Humane Treatment to Lab Animals (2009).

Abbreviations DR, death receptor; MALDI-TOF-MS, matrix assisted laser desorption ionization-time of flight mass spectrometry; MTT, 3-(4,5-dimethylthiazol-2-yl)-2,5-diphenyltetrazolium bromide; PBS, phosphate buffered saline

References

1. Siegel, R., Naishadham, D., Jemal, A.: Cancer statistics, 2013. *CA Cancer J. Clin.* **63**(1):11–30 (2013). <https://doi.org/10.3322/caac.21166>
2. Patrikidou, A., Lorient, Y., Eymard, J.C., Albiges, L., Massard, C., Ileana, E., Di Palma, M., Escudier, B., Fizazi, K.: Who dies from prostate cancer? *Prostate Cancer Prostatic Dis.* **17**(4), 348–352 (2014). <https://doi.org/10.1038/pcan.2014.35>
3. Gundem, G., Van Loo, P., Kremeyer, B., Alexandrov, L.B., Tubio, J.M.C., Papaemmanuil, E., Brewer, D.S., Kallio, H.M.L., Hognas, G., Annala, M., Kivinummi, K., Goody, V., Latimer, C., O'Meara, S., Dawson, K.J., Isaacs, W., Emmert-Buck, M.R., Nykter, M., Foster, C., Kote-Jarai, Z., Easton, D., Whitaker, H.C., Group, I.P., Neal, D.E., Cooper, C.S., Eeles, R.A., Visakorpi, T., Campbell, P.J., McDermott, U., Wedge, D.C., Bova, G.S.: The evolutionary history of lethal metastatic prostate cancer. *Nature* **520**(7547), 353–357 (2015). <https://doi.org/10.1038/nature14347>
4. Munkley, J.: Glycosylation is a global target for androgen control in prostate cancer cells. *Endocr. Relat. Cancer.* **24**(3), R49–R64 (2017). <https://doi.org/10.1530/ERC-16-0569>
5. Munkley, J., Mills, I.G., Elliott, D.J.: The role of glycans in the development and progression of prostate cancer. *Nat Rev Urol.* **13**(6), 324–333 (2016). <https://doi.org/10.1038/nrurol.2016.65>
6. Munkley, J., Vodak, D., Livermore, K.E., James, K., Wilson, B.T., Knight, B., McCullagh, P., McGrath, J., Crundwell, M., Harries, L.W., Leung, H.Y., Robson, C.N., Mills, I.G., Rajan, P., Elliott, D.J.: Glycosylation is an Androgen-Regulated Process Essential for Prostate Cancer Cell Viability. *EBioMedicine.* **8**, 103–116 (2016). <https://doi.org/10.1016/j.ebiom.2016.04.018>
7. Li, Y., Cozzi, P.J.: MUC1 is a promising therapeutic target for prostate cancer therapy. *Curr. Cancer Drug Targets.* **7**(3), 259–271 (2007). <https://doi.org/10.2174/156800907780618338>
8. Pinho, S.S., Reis, C.A.: Glycosylation in cancer: mechanisms and clinical implications. *Nat. Rev. Cancer.* **15**(9), 540–555 (2015). <https://doi.org/10.1038/nrc3982>
9. Drake, R.R.: Glycosylation and cancer: moving glycomics to the forefront. *Adv Cancer Res.* **126**, 1–10 (2015). <https://doi.org/10.1016/bs.acr.2014.12.002>
10. Brockhausen, I., Gao, Y.: Structural Glycobiology. In., pp. 177–214. (2012)
11. Perry, K.M., Onuffer, J.J., Gittelman, M.S., Barmat, L., Matthews, C.R.: Long-range electrostatic interactions can influence the folding, stability, and cooperativity of dihydrofolate reductase. *Biochemistry.* **28**(19), 7961–7968 (1989). <https://doi.org/10.1021/bi00445a061>
12. Holst, S., Wührer, M., Rombouts, Y.: Glycosylation characteristics of colorectal cancer. *Adv Cancer Res.* **126**, 203–256 (2015). <https://doi.org/10.1016/bs.acr.2014.11.004>
13. Vajaria, B.N., Patel, P.S.: Glycosylation: a hallmark of cancer? *Glycoconj J.* **34**(2), 147–156 (2017). <https://doi.org/10.1007/s10719-016-9755-2>
14. Yuan, Q., Chen, X., Han, Y., Lei, T., Wu, Q., Yu, X., Wang, L., Fan, Z., Wang, S.: Modification of alpha2,6-sialylation mediates the invasiveness and tumorigenicity of non-small cell lung cancer cells in vitro and in vivo via Notch1/Hes1/MMPs pathway. *Int J Cancer.* **143**(9), 2319–2330 (2018). <https://doi.org/10.1002/ijc.31737>
15. Burchell, J.M., Beatson, R., Graham, R., Taylor-Papadimitriou, J., Tajadura-Ortega, V.: O-linked mucin-type glycosylation in breast cancer. *Biochem. Soc. Trans.* **46**(4), 779–788 (2018). <https://doi.org/10.1042/BST20170483>
16. Burchell, J., Poulsom, R., Hanby, A., Whitehouse, C., Cooper, L., Clausen, H., Miles, D., Taylor-Papadimitriou, J.: An alpha2,3 sialyltransferase (ST3Gal I) is elevated in primary breast

- carcinomas. *Glycobiology*. **9**(12), 1307–1311 (1999). <https://doi.org/10.1093/glycob/9.12.1307>
17. Wu, X., Zhao, J., Ruan, Y., Sun, L., Xu, C., Jiang, H.: Sialyltransferase ST3GAL1 promotes cell migration, invasion, and TGF-beta1-induced EMT and confers paclitaxel resistance in ovarian cancer. *Cell Death Dis.* **9**(11), 1102 (2018). <https://doi.org/10.1038/s41419-018-1101-0>
18. Chong, Y.K., Sandanaraj, E., Koh, L.W., Thangaveloo, M., Tan, M.S., Koh, G.R., Toh, T.B., Lim, G.G., Holbrook, J.D., Kon, O.L., Nadarajah, M., Ng, I., Ng, W.H., Tan, N.S., Lim, K.L., Tang, C., Ang, B.T.: ST3GAL1-Associated Transcriptomic Program in Glioblastoma Tumor Growth, Invasion, and Prognosis. *J. Natl. Cancer Inst.* **108**(2) (2016). <https://doi.org/10.1093/jnci/djv326>
19. Bai, Q., Liu, L., Xia, Y., Long, Q., Wang, J., Xu, J., Guo, J.: Prognostic significance of ST3GAL-1 expression in patients with clear cell renal cell carcinoma. *BMC Cancer*. **15**, 880 (2015). <https://doi.org/10.1186/s12885-015-1906-5>
20. Yeo, H.L., Fan, T.C., Lin, R.J., Yu, J.C., Liao, G.S., Chen, E.S., Ho, M.Y., Lin, W.D., Chen, K., Chen, C.H., Hung, J.T., Wu, J.C., Chang, N.C., Chang, M.D., Yu, J., Yu, A.L.: Sialylation of vasorin by ST3Gal1 facilitates TGF-beta1-mediated tumor angiogenesis and progression. *Int J Cancer*. **144**(8), 1996–2007 (2019). <https://doi.org/10.1002/ijc.31891>
21. Wen, K.C., Sung, P.L., Hsieh, S.L., Chou, Y.T., Lee, O.K., Wu, C.W., Wang, P.H.: alpha2,3-sialyltransferase type I regulates migration and peritoneal dissemination of ovarian cancer cells. *Oncotarget*. **8**(17), 29013–29027 (2017). <https://doi.org/10.18632/oncotarget.15994>
22. Fan, T.C., Yeo, H.L., Hsu, H.M., Yu, J.C., Ho, M.Y., Lin, W.D., Chang, N.C., Yu, J., Yu, A.L.: Reciprocal feedback regulation of ST3GAL1 and GFRA1 signaling in breast cancer cells. *Cancer Lett.* **434**, 184–195 (2018). <https://doi.org/10.1016/j.canlet.2018.07.026>
23. Li, Y., Luo, S., Dong, W., Song, X., Zhou, H., Zhao, L., Jia, L.: Alpha-2, 3-sialyltransferases regulate the multidrug resistance of chronic myeloid leukemia through miR-4701-5p targeting ST3GAL1. *Lab. Invest.* **96**(7), 731–740 (2016). <https://doi.org/10.1038/labinvest.2016.50>
24. Gao, Y., Chachadi, V.B., Cheng, P.W., Brockhausen, I.: Glycosylation potential of human prostate cancer cell lines. *Glycoconj J.* **29**(7), 525–537 (2012). <https://doi.org/10.1007/s10719-012-9428-8>
25. Morelle, W., Michalski, J.C.: Analysis of protein glycosylation by mass spectrometry. *Nat Protoc.* **2**(7), 1585–1602 (2007). <https://doi.org/10.1038/nprot.2007.227>
26. Robbe, C., Capon, C., Maes, E., Rousset, M., Zweibaum, A., Zanetta, J.P., Michalski, J.C.: Evidence of regio-specific glycosylation in human intestinal mucins: presence of an acidic gradient along the intestinal tract. *J. Biol. Chem.* **278**(47), 46337–46348 (2003). <https://doi.org/10.1074/jbc.M302529200>
27. Robbe-Masselot, C., Herrmann, A., Carlstedt, I., Michalski, J.C., Capon, C.: Glycosylation of the two O-glycosylated domains of human MUC2 mucin in patients transposed with artificial urinary bladders constructed from proximal colonic tissue. *Glycoconj J.* **25**(3), 213–224 (2008). <https://doi.org/10.1007/s10719-007-9079-3>
28. Bae, S., Ma, K., Kim, T.H., Lee, E.S., Oh, K.T., Park, E.S., Lee, K.C., Youn, Y.S.: Doxorubicin-loaded human serum albumin nanoparticles surface-modified with TNF-related apoptosis-inducing ligand and transferrin for targeting multiple tumor types. *Biomaterials*. **33**(5), 1536–1546 (2012). <https://doi.org/10.1016/j.biomaterials.2011.10.050>
29. Wagner, K.W., Punnoose, E.A., Januario, T., Lawrence, D.A., Pitti, R.M., Lancaster, K., Lee, D., von Goetz, M., Yee, S.F., Totpal, K., Huw, L., Katta, V., Cavet, G., Hymowitz, S.G., Amler, L., Ashkenazi, A.: Death-receptor O-glycosylation controls tumor-cell sensitivity to the proapoptotic ligand Apo2L/TRAIL. *Nat Med.* **13**(9), 1070–1077 (2007). <https://doi.org/10.1038/nm1627>
30. Hagiwara, S., Ohyama, C., Takahashi, T., Endoh, M., Moriya, T., Nakayama, J., Arai, Y., Fukuda, M.: Expression of core 2 beta1,6-N-acetylglucosaminyltransferase facilitates prostate cancer progression. *Glycobiology*. **15**(10), 1016–1024 (2005). <https://doi.org/10.1093/glycob/cwi086>
31. Sato, T., Yoneyama, T., Tobisawa, Y., Hatakeyama, S., Yamamoto, H., Kojima, Y., Mikami, J., Mori, K., Hashimoto, Y., Koie, T., Ohyama, C.: Core 2 beta-1, 6-N-acetylglucosaminyltransferase-1 expression in prostate biopsy specimen is an indicator of prostate cancer aggressiveness. *Biochem Biophys Res Commun.* **470**(1), 150–156 (2016). <https://doi.org/10.1016/j.bbrc.2016.01.011>
32. Marcos, N.T., Cruz, A., Silva, F., Almeida, R., David, L., Mandel, U., Clausen, H., Von Mensdorff-Pouilly, S., Reis, C.A.: Polypeptide GalNAc-transferases, ST6GalNAc-transferase I, and ST3Gal-transferase I expression in gastric carcinoma cell lines. *J Histochem Cytochem.* **51**(6), 761–771 (2003). <https://doi.org/10.1177/002215540305100607>
33. Dalziel, M., Whitehouse, C., McFarlane, I., Brockhausen, I., Gschmeissner, S., Schwientek, T., Clausen, H., Burchell, J.M., Taylor-Papadimitriou, J.: The relative activities of the C2GnT1 and ST3Gal-I glycosyltransferases determine O-glycan structure and expression of a tumor-associated epitope on MUC1. *J. Biol. Chem.* **276**(14), 11007–11015 (2001). <https://doi.org/10.1074/jbc.M006523200>
34. Valenzuela, H.F., Pace, K.E., Cabrera, P.V., White, R., Porvari, K., Kaija, H., Vihko, P., Baum, L.G.: O-glycosylation regulates LNCaP prostate cancer cell susceptibility to apoptosis induced by galectin-1. *Cancer Res.* **67**(13), 6155–6162 (2007). <https://doi.org/10.1158/0008-5472.CAN-05-4431>
35. Yoshida, T., Shiraishi, T., Horinaka, M., Wakada, M., Sakai, T.: Glycosylation modulates TRAIL-R1/death receptor 4 protein: different regulations of two pro-apoptotic receptors for TRAIL by tunicamycin. *Oncol. Rep.* **18**(5), 1239–1242 (2007)
36. Mungul, A., Cooper, L., Brockhausen, I., Ryder, K., Mandel, U., Clausen, H., Rugghetti, A., Miles, D.W., Taylor-Papadimitriou, J., Burchell, J.M.: Sialylated core 1 based O-linked glycans enhance the growth rate of mammary carcinoma cells in MUC1 transgenic mice. *Int J Oncol* **25**(4), 937–943 (2004)
37. Picco, G., Julien, S., Brockhausen, I., Beatson, R., Antonopoulos, A., Haslam, S., Mandel, U., Dell, A., Pinder, S., Taylor-Papadimitriou, J., Burchell, J.: Over-expression of ST3Gal-I promotes mammary tumorigenesis. *Glycobiology*. **20**(10), 1241–1250 (2010). <https://doi.org/10.1093/glycob/cwq085>
38. Wu, H., Shi, X.L., Zhang, H.J., Song, Q.J., Yang, X.B., Hu, W.D., Mei, G.L., Chen, X., Mao, Q.S., Chen, Z.: Overexpression of ST3Gal-I promotes migration and invasion of HCCLM3 in vitro and poor prognosis in human hepatocellular carcinoma. *Oncotargets Ther.* **9**, 2227–2236 (2016). <https://doi.org/10.2147/OTT.S96510>

Publisher's note Springer Nature remains neutral with regard to jurisdictional claims in published maps and institutional affiliations.